

Vision-Language Attribute Disentanglement and Reinforcement for Lifelong Person Re-Identification

Kunlun Xu^{1*} Haotong Cheng^{1*} Jiangmeng Li² Xu Zou³ Jiahuan Zhou^{1†}

¹ Wangxuan Institute of Computer Technology, Peking University, Beijing, China

² University of Chinese Academy of Sciences, Beijing, China

³ School of Artificial Intelligence and Automation, Huazhong University of Science and Technology, Wuhan, China

xkl@stu.pku.edu.cn chenght9923@mails.jlu.edu.cn jiangmeng2019@iscas.ac.cn zoux@hust.edu.cn jiahuanzhou@pku.edu.cn

Abstract

Lifelong person re-identification (LReID) aims to learn from varying domains to obtain a unified person retrieval model. Existing LReID approaches typically focus on learning from scratch or a visual classification-pretrained model, while the Vision-Language Model (VLM) has shown generalizable knowledge in a variety of tasks. Although existing methods can be directly adapted to the VLM, since they only consider global-aware learning, the fine-grained attribute knowledge is underleveraged, leading to limited acquisition and anti-forgetting capacity. To address this problem, we introduce a novel VLM-driven LReID approach named Vision-Language Attribute Disentanglement and Reinforcement (VLADR). Our key idea is to explicitly model the universally shared human attributes to improve inter-domain knowledge transfer, thereby effectively utilizing historical knowledge to reinforce new knowledge learning and alleviate forgetting. Specifically, VLADR includes a Multi-grain Text Attribute Disentanglement mechanism that mines the global and diverse local text attributes of an image. Then, an Inter-domain Cross-modal Attribute Reinforcement scheme is developed, which introduces cross-modal attribute alignment to guide visual attribute extraction and adopts inter-domain attribute alignment to achieve fine-grained knowledge transfer. Experimental results demonstrate that our VLADR outperforms the state-of-the-art methods by 1.9%-2.2% and 2.1%-2.5% on anti-forgetting and generalization capacity. Our source code is available at <https://github.com/zhoujiahuan1991/CVPR2026-VLADR>.

1. Introduction

Person re-identification (ReID) aims to retrieve the same individual across non-overlapping camera views [5, 9, 32].

*Equal contribution

†Corresponding author

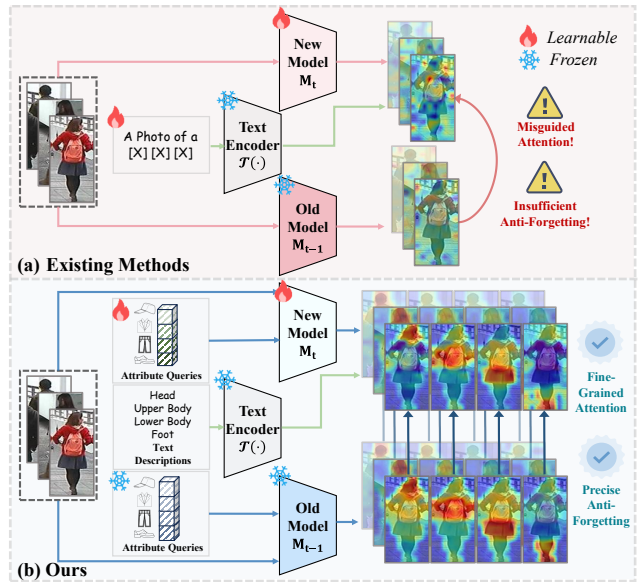


Figure 1. (a) Existing methods rely on global feature learning when exploiting VLM, suffering from misguided attention on background and insufficient utilization of the human semantics. (b) Our method explicitly models and transfers human attribution knowledge across domains, achieving more precise human semantic acquisition and continual attribute knowledge reinforcement.

While conventional ReID methods primarily address the stationary scenarios [10], real-world deployments often operate in dynamic settings where data continuously stream in under varying weather, illumination, and resolution domains [8, 38, 44, 46, 50]. To close the gap, lifelong person re-identification (LReID) [6, 40, 41] has emerged as a promising research direction. The primary challenge in LReID lies in the continuous integration of domain-specific knowledge to construct a universal model that remains robust and adaptable to evolving conditions [7, 42].

Existing LReID approaches primarily follow a conventional learning paradigm, in which models are either trained from scratch or initialized with a visually pre-trained clas-

sification backbone [17, 30]. However, owing to the lack of human-centric prior knowledge, these methods often suffer from limited robustness and generalization capability [14].

Recent advances have demonstrated remarkable generalization capabilities of Vision-Language Models (VLMs) across various visual tasks, including ReID [14, 18, 48]. Although existing LReID methods can be integrated into a VLM-based baseline, as shown in Fig. 1 (a), they predominantly rely on global-aware learning with coarse supervision. Such supervision often causes the model to overfit to irrelevant regions, such as background objects, instead of focusing on person-specific regions. Consequently, these learning paradigms misguide the knowledge accumulation process and hinder the acquisition of new information, ultimately degrading model robustness.

To address these limitations, we propose a novel framework termed **V**ision-**L**anguage **A**tribute **D**isentanglement and **R**einforcement (VLADR). As illustrated in Fig. 1 (b), the central idea of VLADR is to disentangle universally shared human attributes to achieve more precise and human-centric knowledge representation. This design enables effective transfer of human-relevant historical knowledge to new domains, thereby continually reinforcing fine-grained attribute knowledge. Specifically, VLADR consists of two main components: a Multi-grain Text Attribute Disentanglement (MTAD) mechanism and an Inter-domain Cross-modal Attribute Reinforcement (ICAR) scheme. MTAD extracts both global and diverse local textual attributes from images based on a pretrained VLM. Building upon these disentangled attributes, ICAR conducts cross-modal attribute alignment to enable fine-grained visual attribute learning. In addition, an inter-domain attribute alignment strategy is introduced to facilitate attribute knowledge transfer and retention across domains. Through the joint operation of MTAD and ICAR, human-relevant attribute knowledge is progressively reinforced throughout sequential training. Extensive experiments demonstrate that VLADR substantially enhances both knowledge acquisition and knowledge consolidation in LReID.

In summary, the contributions of this work are three-fold: (1) We present a pioneering study that leverages VLMs for lifelong person re-identification and propose the novel VLADR framework that effectively utilizes multi-granularity human-centric knowledge to facilitate knowledge acquisition while mitigating catastrophic forgetting. (2) We develop a Multi-grain Text Attribute Disentanglement (MTAD) mechanism that extracts diverse coarse- and fine-grained textual attributes, coupled with an Inter-domain Cross-modal Attribute Reinforcement (ICAR) scheme that continuously reinforces visual attribute knowledge across domains throughout the lifelong learning process. (3) Extensive experiments demonstrate that our VLADR achieves state-of-the-art performance.

2. Related Work

2.1. Lifelong Person Re-Identification

Person Re-Identification (ReID) aims to match individuals across non-overlapping camera views. While conventional methods predominantly operated under the assumption that training and testing data originated from the same domain [22, 28]. This premise significantly limited their practicality in real-world surveillance systems, where environmental conditions are inherently dynamic [2, 12, 54]. To overcome this limitation, Lifelong Person Re-Identification (LReID) has emerged as a promising paradigm, aiming to learn continuously from a sequential stream of domains. The central challenge in LReID is catastrophic forgetting, a tendency where models overwrite old knowledge when learning from new domains [24, 33]. Existing LReID approaches could be broadly categorized into exemplar-based and exemplar-free methods [42].

Exemplar-based methods alleviated forgetting by storing representative samples from past domains (exemplars) and replaying them during subsequent training [8, 38, 49]. Although these methods often yielded strong performance, they incurred linearly increasing storage and computational overhead. More critically, the storage of raw human images raised substantial privacy concerns, hindering their deployment in real-world scenarios [40, 53]. Consequently, our work focuses on the more challenging and practical exemplar-free setting.

Existing exemplar-free methods primarily mitigated forgetting through techniques such as knowledge distillation, prototype learning, and style transfer. Knowledge distillation-based approaches enforced consistency between historical and current model outputs [30, 34, 42, 44]. Prototype-based methods [41, 53] introduced prototypes to preserve historical information. Style transfer-based techniques replicated visual styles from previous domains to enhance knowledge retention [43]. However, these methods typically either learned from scratch or initialized with a generic classification-pretrained model [4, 30], thereby lacking explicit human-centric prior knowledge. This fundamental limitation restricted their capacity to learn discriminative representations robust to domain shifts and long-term forgetting [36].

2.2. VLM-based Person Re-Identification

VLMs acquired extensive real-world knowledge during pre-training and have demonstrated significant potential in enhancing various vision tasks [29, 50]. In light of this, several works have attempted to leverage VLM for person re-identification [3, 14, 18, 48]. These methods typically imposed a global alignment constraint during downstream ReID training, maintaining the original vision-language alignment architecture. However, such coarse-grained con-

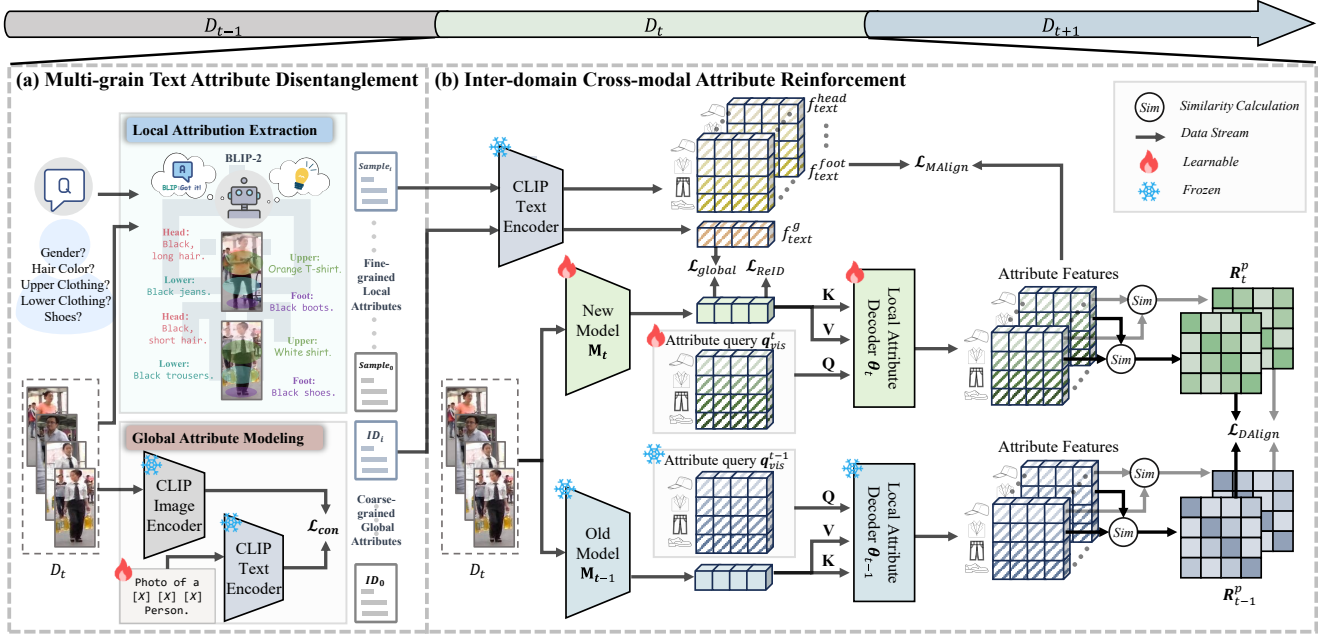


Figure 2. Overview of our framework. Given the new data D_t , two stages operate sequentially. (a) Multi-grain Text Attribute Disentanglement mechanism conducts local attribution extraction and a global attribute model based on pretrained VLMs. Then, these disentangled multi-grain attributes are utilized by (b) Inter-domain Cross-modal Attribute Reinforcement scheme, which conducts visual-text alignment \mathcal{L}_{MAlign} to guide visual attribute extraction. Besides, the inter-domain attribute alignment \mathcal{L}_{DAlign} is also performed to accumulate the continually learned knowledge.

straints failed to guide the model to precisely and comprehensively extract the human-relevant information. As a consequence, the noise-prone features accumulated progressively during lifelong learning, which disrupted effective knowledge acquisition and undermined model robustness [40, 42]. Moreover, incompletely learned features limited the utilization of new training data. To overcome these limitations, we investigate guiding the model in learning diverse human attributes grounded in VLM knowledge, thereby facilitating both robust feature representation and reliable long-term knowledge accumulation.

3. The Proposed Method

3.1. Problem Definition

LReID addresses the scenarios where a stream of training datasets $\mathcal{D} = \{D_t\}_{t=1}^T$ are provided incrementally, and each dataset $D_t = \{(x_i, y_i)\}_{i=1}^{n_t}$ consists of n_t image-label pairs with x_i being an image and y_i its corresponding identity label. When D_t is presented for training, all previous datasets D_1, \dots, D_{t-1} are inaccessible [41]. After the t -th training step, the final model is denoted as M_t , which is evaluated on T test datasets $\mathcal{D}^{te} = \{D_t^{te}\}_{t=1}^T$ drawn from T identical training domains. Additionally, U unseen datasets $\mathcal{D}^{un} = \{D_t^{un}\}_{t=1}^U$ collected from novel domains are employed to evaluate the generalization capacity of M_T .

3.2. Overview

As illustrated in Fig. 2, our framework consists of two core stages: Multi-grain Text Attribute Disentanglement (MTAD) and Inter-domain Cross-modal Attribute Reinforcement (ICAR). Given incoming data D_t , MTAD first leverages BLIP to generate part-wise textual attribute descriptions for each instance, while simultaneously utilizing CLIP to extract ReID-aware global attributes. Subsequently, ICAR encodes these multi-grain textual attribute features through the CLIP text encoder. Visual global and local attribute features are then extracted and aligned with their textual counterparts through cross-modal alignment. Additionally, to facilitate knowledge accumulation across domains, an inter-domain attribute knowledge alignment mechanism is developed to achieve knowledge transfer.

3.3. Multi-grain Text Attribute Disentanglement

In standard LReID benchmarks, only the human images and the corresponding identity labels are provided. Therefore, to effectively leverage the semantic knowledge in VLMs, generating an appropriate textual description becomes crucial. In this section, we introduce how to generate the local and global text attributes without using auxiliary data.

Local Attribution Extraction. Recent advancements in image-to-text generation models have demonstrated remarkable capabilities for producing human descriptions.

However, existing approaches typically generate only a single paragraph or phrase per sample [35, 47]. Such strategies fail to capture fine-grained information, leading to limited knowledge acquisition capacity, as shown in Fig. 1 (a).

To address this issue, we disentangle the human body into distinct local semantic regions, including head, upper body, lower body and foot. A set of textual queries $\mathcal{Q} = \{T_i^Q\}_{i=1}^{N_a}$ are predefined, with each targeting a specific local attribute. Given an input image, the corresponding attribute T_i^A is extracted by the BLIP model \mathcal{B} as following:

$$T_{x,i}^A = \mathcal{B}(x, T_i^Q). \quad (1)$$

Consequently, a set of local textual semantic attributes $\mathcal{T}_x = \{T_{x,i}^A\}_{i=1}^{N_a}$ is obtained according to Eq. 1. \mathcal{T}_x provides a precise description of human parts. It is worth noting that excessively fine-grained local attributes do not necessarily yield better performance, and the detailed configurations of selected local attributes and \mathcal{Q} are provided in our Supplementary Materials.

Global Attribute Modeling. In addition to local attributes, we introduce global attribute modeling to provide complementary semantic information, enabling more comprehensive human characterization. Inspired by [18], we extract the ReID-aware global attribute based on the CLIP model. Specifically, a set of learnable text prompts $\{[X]_i\}_{i=1}^M$ are assigned to each identity. The input image x and the corresponding text description ‘‘A photo of a $[X]_1[X]_2[X]_3 \dots [X]_M$ ’’ are fed into the frozen image encoder $\mathcal{I}(\cdot)$ and text encoder $\mathcal{T}(\cdot)$, respectively. The text prompts are optimized by minimizing:

$$\mathcal{L}_{prompt} = \sum_x \mathcal{L}_{i2t}(x) + \sum_x \mathcal{L}_{t2i}(x), \quad (2)$$

where \mathcal{L}_{i2t} and \mathcal{L}_{t2i} denote the contrastive loss items as depicted in [18]. To preserve the generalizable knowledge in CLIP, both $\mathcal{I}(\cdot)$ and $\mathcal{T}(\cdot)$ remain frozen as the training stage t increases.

3.4. Inter-domain Cross-modal Attribute Reinforcement

In this section, we aim to mine and accumulate visual knowledge throughout the lifelong learning process. Specifically, three learning branches are introduced: Coarse-grained Global Representation Learning, Fine-grained Local Attribute Mining, and Inter-domain Attribute Knowledge Transfer.

Coarse-grained Global Representation Learning.

Given a batch of B input samples $\{(x_i, y_i)\}_{i=1}^B$, we employ a ViT-based visual model \mathbf{M}_t to extract features from each instance x_i . Specifically, x_i is tokenized [17] into a sequence represented as $\mathbf{f}_t^i \in \mathbb{R}^{L_h \times d}$, where L_h and d are the sequence length and token dimension, respectively. Additionally, a [CLS] token \mathbf{f}_{cls}^i is attached to \mathbf{f}_t^i , resulting in

a sequence $\mathbf{h}_t^i = [\mathbf{f}_t^i, \mathbf{f}_{cls}^i]$. After processed by \mathbf{M}_t , \mathbf{f}_{cls}^i is treated as the global vision feature $\mathbf{f}_{vis}^{g,i}$. Following previous works [41, 42], the classical ReID loss \mathcal{L}_{ReID} is adopted to ensure knowledge learning, which is defined as:

$$\mathcal{L}_{ReID} = \mathcal{L}_{Tri} + \mathcal{L}_{ce}, \quad (3)$$

where \mathcal{L}_{Tri} and \mathcal{L}_{ce} are the triplet loss [15] and a cross-entropy loss [41].

Subsequently, the text prompt corresponding to identity y_i is utilized to generate the textual global attribute feature $\mathbf{f}_{text}^{g,i}$. To establish cross-modal correspondence, the visual-text global attribute alignment loss is conducted:

$$\mathcal{L}_{global} = -\frac{1}{B} \sum_{i=1}^B \log \frac{\exp(s(\mathbf{f}_{vis}^{g,i}, \mathbf{f}_{text}^{g,i}))}{\sum_{k=1}^K \exp(s(\mathbf{f}_{vis}^{g,i}, \mathbf{f}_{text}^{g,k}))}, \quad (4)$$

where $s(\cdot, \cdot)$ is the cosine similarity.

Fine-grained Local Attribute Mining. While MTAD enables the extraction of multi-grain textual attributes, corresponding visual attributes still remain unavailable due to the prohibitive annotation cost in LReID settings. To overcome this limitation, we introduce an adaptive visual attribute learning paradigm. Specifically, a set of N_a learnable attribution query $\mathbf{q}_{vis} \in \mathbb{R}^{N_a \times d}$ is defined, each corresponding to a local attribute defined in Sec. 3.3.

Then, a Local Attribute Decoder θ_t , implemented as a cross attention layer, is employed to decode the visual attributes. Specifically, the image token sequence \mathbf{f}_t^i serves as the Key (\mathbf{K}) and value (\mathbf{V}). \mathbf{q}_{vis} is adopted as Query (\mathbf{Q}). The visual local attribute features $F_{vis}^{l,t}$ are thus computed as:

$$F_{vis}^{l,t} = \theta_t(\mathbf{q}_{vis}, \mathbf{f}_t^i, \mathbf{f}_t^i). \quad (5)$$

On the textual side, the CLIP text encoder processes the local attributes \mathcal{T}_{x_i} generated in Sec. 3.3, obtaining the textual local attribute features $F_{text}^{l,t} \in \mathbb{R}^{N_a \times d}$:

$$F_{text}^{l,t} = \mathcal{T}(\mathcal{T}_{x_i}). \quad (6)$$

The visual-text local attribute alignment is then optimized through:

$$\mathcal{L}_{MA} = \frac{1}{N_a} \sum_{p=1}^{N_a} \mathcal{L}_{cons}^p, \quad (7)$$

where \mathcal{L}_{cons}^p denotes the contrastive loss for single attribute. Inspired by [18, 26], \mathcal{L}_{cons}^p is defined as:

$$\mathcal{L}_{cons}^p = -\frac{1}{2B} \sum_{i=1}^B \left(\log \frac{\exp(s(\mathbf{v}_i^{p,t}, \mathbf{t}_i^{p,t}))}{\sum_{j=1}^B \exp(s(\mathbf{v}_i^{p,t}, \mathbf{t}_j^{p,t}))} + \log \frac{\exp(s(\mathbf{v}_i^{p,t}, \mathbf{t}_i^{p,t}))}{\sum_{k=1}^B \exp(s(\mathbf{v}_k^{p,t}, \mathbf{t}_i^{p,t}))} \right), \quad (8)$$

Table 1. Comparison results of Seen-domain anti-forgetting and UnSeen-domain generalization on Training Order-1.

Net.	Method	Pub.	Market		SYSU		LPW		MSMT17		CUHK03		Seen-Avg		Unseen-Avg	
			mAP	R@1	mAP	R@1	mAP	R@1	mAP	R@1	mAP	R@1	mAP	R@1	mAP	R@1
ResNet	LwF[24]	TPAMI 2017	44.4	68.7	66.6	69.8	25.0	36.0	6.8	19.6	52.9	53.6	39.1	49.5	50.9	43.8
	DKP[41]	CVPR 2024	60.0	80.3	84.1	85.9	46.0	57.9	17.7	38.5	41.0	41.4	49.8	60.8	57.5	50.7
	LSTKC[42]	AAAI 2024	57.0	78.6	82.9	84.9	47.2	58.4	18.4	41.1	42.3	43.7	49.6	61.3	57.8	50.2
	DKP++[53]	TPAMI 2025	52.1	76.5	75.6	77.7	45.2	58.1	14.9	36.1	40.1	42.2	45.6	58.1	56.6	48.5
	LSTKC++[44]	TPAMI 2025	67.5	83.9	86.3	88.2	52.1	61.9	19.4	40.3	47.0	47.8	54.5	64.4	62.9	55.6
	DASK[43]	AAAI 2025	49.3	74.0	74.9	77.0	45.7	58.6	17.6	42.0	34.5	35.6	44.4	57.5	59.6	52.5
ViT	PAEMA[17]	IJCV 2024	73.1	88.0	90.0	91.5	59.5	68.6	30.4	54.4	48.4	48.4	60.3	70.2	69.8	63.2
	DRE[25]	TNNLS 2025	61.7	80.8	88.0	89.8	52.6	64.7	32.0	57.3	59.4	61.3	58.7	70.8	62.9	58.1
CLIP	LwF[24]	TPAMI 2017	51.4	77.6	73.6	76.5	36.3	46.9	13.7	35.0	27.2	26.0	40.4	52.4	55.0	47.1
	DKP†[41]	CVPR 2024	81.1	91.4	90.0	91.0	66.9	74.4	37.4	63.6	59.5	62.0	67.0	76.5	72.5	64.9
	LSTKC†[42]	AAAI 2024	79.8	91.4	92.0	92.7	65.8	75.1	37.8	63.5	60.6	62.4	67.2	77.0	75.3	68.5
	PAEMA†[17]	IJCV 2024	81.3	92.1	92.2	93.0	66.9	75.4	39.2	65.4	58.3	60.3	67.6	77.2	75.6	69.8
	DKP++†[53]	TPAMI 2025	79.4	90.5	87.8	88.5	66.1	74.6	37.7	64.2	57.9	59.3	65.8	75.4	73.0	66.2
	LSTKC++†[44]	TPAMI 2025	69.3	85.5	89.9	90.9	60.3	71.4	38.3	64.0	69.1	70.4	65.4	76.4	74.1	67.7
	DASK†[43]	AAAI 2025	79.7	90.7	91.0	91.7	64.7	73.9	42.1	67.9	63.4	65.5	68.2	78.0	74.2	66.7
	VLADR	<i>This Paper</i>	80.1	91.9	92.0	92.5	67.8	76.2	45.5	70.5	66.6	68.4	70.4	79.9	77.8	72.0

Net. represents the Backbone network. † indicates integrating the LReID approach with CLIP-ReID [18] baseline.

where $\mathbf{v}^{p,t} \in \mathbb{R}^{B \times d}$ and $\mathbf{t}^{p,t} \in \mathbb{R}^{B \times d}$ represent visual and textual features of attribute p across the batch, extracted from $F_{vis}^{l,t}$ and $F_{text}^{l,t}$ respectively.

Inter-domain Attribute Knowledge Transfer. To facilitate the transfer of previously learned attribute knowledge to the current model, we leverage the frozen visual model \mathbf{M}_{t-1} , attribute query \mathbf{q}_{vis}^{t-1} , and local attribute decoder θ_{t-1} to process each input sample x_i , generating the historical visual local attribute features $F_{vis}^{l,t-1} \in \mathbb{R}^{N_a \times d}$. Let $\mathbf{v}^{p,t-1} \in \mathbb{R}^{B \times d}$ denote the historical features of attribute p in a batch, extracted from $F_{vis}^{l,t-1}$. Following [43], the cross-instance relation matrices $\mathbf{R}_{t-1}^p = \gamma(\mathbf{v}^{p,t-1}(\mathbf{v}^{p,t-1})^\top)$ and $\mathbf{R}_t^p = \gamma(\mathbf{v}^{p,t}(\mathbf{v}^{p,t})^\top)$ are calculated, where $\gamma(\cdot)$ is a row-wise normalization operator. Finally, the inter-domain attribute alignment loss is then defined as

$$\mathcal{L}_{DAlign} = \frac{1}{N_a} \sum_{p=1}^{N_a} \mathcal{L}_{Rel}^p, \quad (9)$$

where \mathcal{L}_{Rel}^p is a Kullback-Leibler (KL) divergence-based relation distillation loss calculated by:

$$\mathcal{L}_{Rel}^p = \frac{1}{B} \sum_{i=1}^B KL\left(\left(\mathbf{R}_t^p\right)_i \parallel \left(\mathbf{R}_{t-1}^p\right)_i\right), \quad (10)$$

Training and Inference. During the MTAD stage (Sec. 3.3), only Eq. (2) is optimized. In the ICAR stage, the overall loss \mathcal{L} is combined as:

$$\mathcal{L} = \mathcal{L}_{ReID} + \mathcal{L}_{global} + \alpha \mathcal{L}_{MAAlign} + \beta \mathcal{L}_{DAlign}, \quad (11)$$

where α and β are hyperparameters to balance different loss components.

During inference, the final visual model \mathbf{M}_T , local attribute query \mathbf{q}_{vis}^T and local attribute decoder θ_T are adopted for feature extraction. Specifically, given an input image x , the global feature f_{vis}^g extracted by \mathbf{M}_T and the visual local attribute features $F_{vis}^{l,T}$ extracted by θ_T and \mathbf{q}_{vis}^T , form the final feature:

$$f_{vis}^c = [f_{vis}^g, F_{vis}^{l,T}]. \quad (12)$$

This comprehensive feature vector f_{vis}^c is subsequently adopted for person retrieval.

4. Experiments

4.1. Datasets and Evaluation Metrics

Datasets: Following previous works [34, 42], all experiments are conducted on the standard LReID benchmark. Since the DukeMTMC-reID [31] dataset in the original benchmark has been officially withdrawn, we follow [45] and adopt LPW_s2 as its replacement. The benchmark consists of 12 dataset subsets in total, among which 5 are used for training (Market-1501 [52], LPW_s2 [45], CUHK-SYSU [39], MSMT17-V2 [37], CUHK03 [21]), while the remaining 7 datasets are used exclusively for evaluation (CUHK01 [20], CUHK02 [19], VIPeR [11], PRID [13], iLIDS [1], GRID [27], SenseReID [51]). In accordance with the established LReID protocols [34], two distinct training

Table 2. Comparison results of Seen-domain anti-forgetting and UnSeen-domain generalization on Training Order-2.

Net.	Method	Pub.	LPW		MSMT17		Market		SYSU		CUHK03		Seen-Avg		Unseen-Avg	
			mAP	R@1	mAP	R@1	mAP	R@1	mAP	R@1	mAP	R@1	mAP	R@1	mAP	R@1
ResNet	LwF[24]	<i>TPAMI 2017</i>	38.8	50.5	6.7	19.2	43.9	67.1	73.2	75.9	50.1	51.9	42.5	52.9	50.0	42.7
	DKP[41]	<i>CVPR 2024</i>	49.5	61.4	14.1	32.6	60.3	80.6	84.5	86.4	43.6	43.7	50.4	60.9	59.5	52.4
	LSTKC[42]	<i>AAAI 2024</i>	46.7	57.6	14.9	33.9	56.5	78.0	84.0	86.1	42.1	43.7	48.8	59.9	57.4	49.5
	DKP++[53]	<i>TPAMI 2025</i>	52.2	64.0	18.0	41.0	63.7	82.5	81.3	82.9	49.7	51.8	53.0	64.4	61.0	54.0
	LSTKC++[44]	<i>TPAMI 2025</i>	55.7	65.7	15.0	34.3	66.9	83.6	86.3	87.6	48.4	49.9	54.4	64.2	63.4	56.0
	DASK[43]	<i>AAAI 2025</i>	47.2	60.4	16.1	39.9	58.7	79.9	77.5	79.4	42.0	43.0	48.3	60.5	60.0	52.8
ViT	PAEMA[17]	<i>IJCV 2024</i>	64.7	73.9	26.5	50.0	73.5	87.6	90.6	91.5	48.9	49.4	60.9	70.5	70.5	63.8
	DRE[25]	<i>TNNLS 2025</i>	42.2	52.3	23.6	45.8	68.2	84.3	87.3	89.1	51.9	53.2	54.6	64.9	60.0	54.4
CLIP	LwF[24]	<i>TPAMI 2017</i>	46.8	59.1	9.4	25.8	50.0	73.9	79.7	82.0	27.1	26.7	42.6	53.5	52.8	45.4
	DKP [†] [41]	<i>CVPR 2024</i>	70.2	77.5	35.7	62.1	80.0	90.7	90.9	91.5	61.9	64.0	67.7	77.2	73.9	66.7
	LSTKC [†] [42]	<i>AAAI 2024</i>	69.2	77.6	34.4	60.7	74.9	88.6	92.8	93.7	60.4	61.9	66.3	76.5	74.5	68.2
	PAEMA [†] [17]	<i>IJCV 2024</i>	71.2	79.2	32.4	58.8	78.1	90.5	92.9	93.5	57.7	58.2	66.5	76.0	75.3	68.8
	DKP++ [†] [53]	<i>TPAMI 2025</i>	69.1	77.5	35.3	61.9	78.6	89.9	88.5	89.2	58.9	60.5	66.1	75.8	73.2	66.6
	LSTKC++ [†] [44]	<i>TPAMI 2025</i>	60.7	71.0	34.5	60.6	73.3	87.0	92.1	93.0	70.6	72.9	66.2	76.9	76.0	69.7
	DASK [†] [43]	<i>AAAI 2025</i>	68.7	77.4	39.1	65.2	77.7	89.5	91.8	92.4	63.7	65.2	68.2	77.9	75.9	68.8
	VLADR	<i>This Paper</i>	69.5	77.4	40.8	67.1	80.6	91.3	92.9	93.6	67.9	69.6	70.3	79.8	78.1	72.2

Net. represents the Backbone network. [†] indicates integrating the LReID approach with CLIP-ReID [18] baseline.

orders are adopted to simulate different domain gaps ^{1 2}. The detailed configurations of the datasets are provided in our Supplementary Material.

Besides, since several closed-source methods have only reported results on the benchmark that contains DukeMTMC-reID, we also provide a comparison with these methods in the Supplementary Material for a comprehensive evaluation.

Evaluation Metrics: Following previous LReID studies [30, 34, 41], we adopt mean Average Precision (mAP) and Rank-1 accuracy (R@1) to evaluate model performance across different domains. In addition, we report the average mAP and R@1 over all training (Seen-Avg) and novel (Unseen-Avg) domains to comprehensively assess the model’s anti-forgetting ability and generalization performance, respectively.

4.2. Implementation Details

Our implementation builds upon the framework of [18], utilizing ViT-B/16 as the visual backbone. BLIP-2 [16] is employed as the image description generator. For MTAD, the training configuration is consistent with [18]. For ICAR, the first dataset is trained for 80 epochs, and each subsequent dataset is trained for 60 epochs. The mini-batch size is set to 64, comprising 32 identities with 4 images per identity.

¹(Order-1) Market-1501→CUHK-SYSU→LPW_s2→MSMT17→CUHK03

²(Order-2) LPW_s2→MSMT17→Market-1501→CUHK-SYSU→CUHK03

All input images are resized to 256×128 . The hyperparameters α and β are both set to 1.0 by default. All experiments are conducted on two NVIDIA RTX 4090 GPUs.

4.3. Compared Methods

We compare the proposed VLADR with three categories of LReID models according to their backbone architectures: A. *ResNet-based models*, including LwF [23], DKP [41], LSTKC [42], DKP++ [53], LSTKC++ [44], and DASK [43]; B. *ViT-based models*, including PAEMA [17] and DRE [25]; C. *CLIP-based models*, obtained by integrating the CLIP-ReID baseline with state-of-the-art LReID methods. All experimental results are either directly reported from official publications or reproduced using the released implementations.

The performance of all compared methods is summarized in Tab. 1 and Tab. 2, corresponding to training order-1 and order-2, respectively. Results on individual seen domains, average performance across all seen domains (Seen-Avg), and unseen domains (Unseen-Avg) are presented, with the best and second-best results highlighted in **Red** and **Blue**, respectively.

4.4. Seen-Domain Performance Evaluation

Compared to ResNet/ViT-based Methods: As shown in Tab. 1 and Tab. 2, VLADR consistently outperforms state-of-the-art ResNet-based and ViT-based approaches across all seen domains. Under Training Order-1, VLADR achieves improvements of **15.9%/15.5%** in Seen-Avg

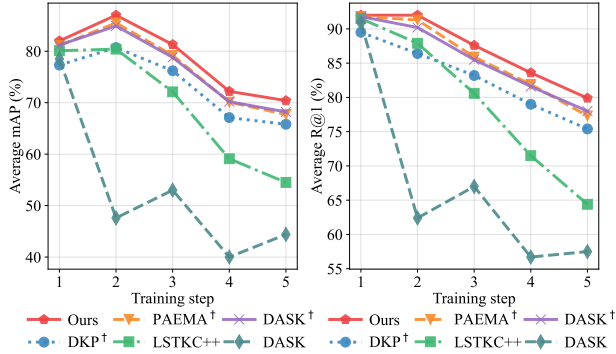


Figure 3. Tendency on seen domain knowledge accumulation.

mAP/R@1, and **10.1%/9.1%**. Under Training Order-2, these gains arise because ResNet/ViT-based methods rely on ImageNet-pretrained classification models, whose lack of human-centric priors limits their ability to learn discriminative features. In contrast, our VLM-driven framework effectively leverages the abundant pretrained knowledge embedded in VLMs, which substantially enhances feature extraction during the lifelong learning process.

Compare to CLIP-based Methods: As shown in Tab. 1 and Tab. 2, integrating existing ResNet/ViT-based approaches into the CLIP-ReID [18] baseline generally leads to noticeable performance improvements, with DASK† achieving the best results among them due to its historical style data generation mechanism. Nevertheless, VLADR surpasses DASK† by **2.2%/1.9%** and **2.1%/1.9%** in Seen-Avg mAP/R@1 across the two training orders. These improvements stem from our attribute disentanglement and reinforcement paradigm, which effectively exploits the human-centric priors within VLMs to enhance human feature parsing and guide the model toward more comprehensive extraction and consolidation of discriminative knowledge across domains.

Furthermore, the learnable text prompts, attribute queries, and local attribute decoder introduced in VLADR are lightweight, adding only marginal computational overhead. In contrast, DASK† requires an additional data generation module and significantly enlarges the training set. Therefore, compared with DASK†, our VLADR is both more **effective** and more **efficient**.

Seen-Domain Performance Tendency: Fig. 3 illustrates the seen-domain performance trends throughout the sequential training process. At the initial training step, our method exhibits a slight advantage in mAP over all existing approaches. This improvement arises from the attribute disentanglement and visual-text local attribute alignment mechanisms, which enhance the model’s ability to acquire discriminative knowledge. As training proceeds and more domains are introduced, the performance gap be-

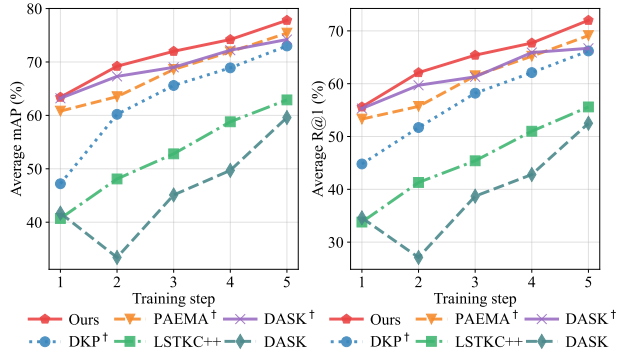


Figure 4. Tendency on unseen domain generalization.

tween VLADR and existing methods continues to widen. This consistent improvement is primarily attributed to the inter-domain attribute knowledge alignment design, which enables reliable knowledge accumulation and facilitates attribute knowledge reinforcement across domains.

4.5. Unseen-Domain Generalization Evaluation

Compared to ResNet/ViT/CLIP-based Methods: As shown in Tab. 1, VLADR surpasses all compared methods by at least **14.9%/16.4%** in Unseen-Avg mAP/R@1 when compared to ResNet-based models, and by **8.0%/8.8%** relative to ViT-based approaches. For CLIP-based models, the minimum improvement is **2.2%/2.2%**. Likewise, under Training Order-2 (Tab. 2), VLADR consistently outperforms all ResNet/ViT/CLIP-based methods, achieving margins of at least **2.1%/2.5%** in Unseen-Avg mAP/R@1. These substantial improvements stem from the proposed attribute disentanglement and reinforcement mechanisms, which guide the model to learn universally discriminative and domain-invariant features that generalize effectively to unseen environments.

Unseen-Domain Performance Tendency: As presented in Fig. 4, our VLADR exhibits comparable generalization ability to DASK† at the initial training step, and consistently outperforms all existing methods as training progresses. This trend demonstrates that the proposed vision-language attribute disentanglement and reinforcement paradigm enables the continual accumulation of universal, transferable knowledge throughout the learning process.

Attention Map visualization: To further demonstrate the superiority of the proposed fine-grained attribute modeling mechanism, we visualize the attention maps generated by each local attribute query, as well as their combined attention map. For comparison, global attention maps from existing approaches are also included. The results in Fig. 5 show that each local attribute query accurately captures part-level semantics, and their combination yields a comprehensive representation of human information. In

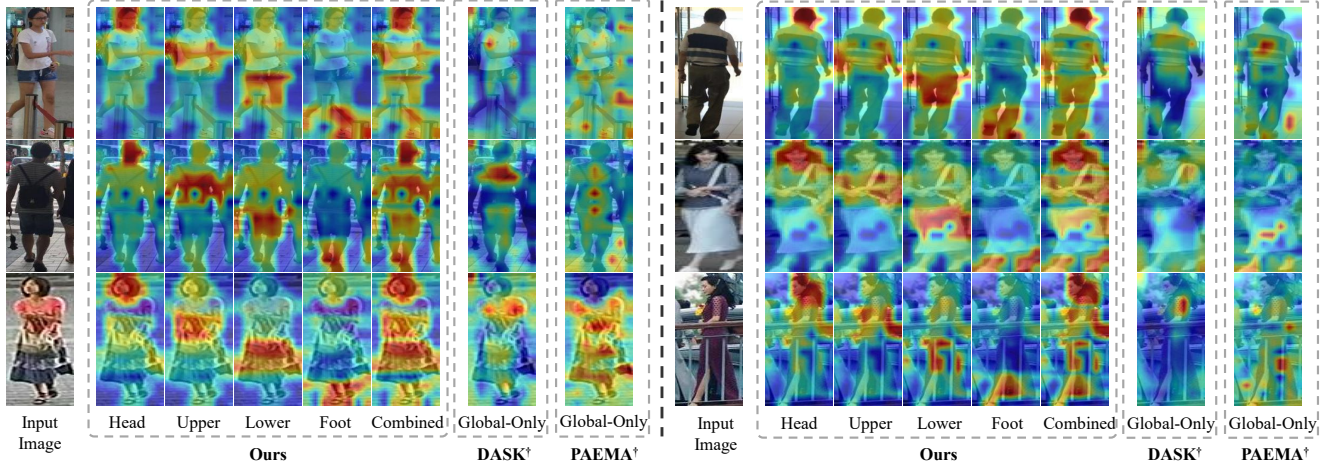


Figure 5. Attention map comparison across different approaches.

Table 3. Ablation on the proposed model components.

Baseline	\mathcal{L}_{MAlign}	\mathcal{L}_{DAlign}	Seen-Avg mAP	Seen-Avg R@1	Unseen-Avg mAP	Unseen-Avg R@1
✓			57.1	66.6	66.4	58.8
✓	✓		66.3	75.8	74.6	68.0
✓	✓	✓	70.4	79.9	77.8	72.0

contrast, existing methods highlight only partial human regions or undesirably attend to background areas, reflecting their limited capacity for precise semantic extraction.

4.6. Ablation Studies

We perform ablation studies on the components proposed under Training Order-1 as follows:

Ablations on model components: As shown in Tab. 3, the baseline is the CLIP-ReID [18] framework trained with $\mathcal{L}_{ReID} + \mathcal{L}_{global}$. When incorporating \mathcal{L}_{MAlign} , both the Multi-grain Text Attribute Disentanglement module and \mathcal{L}_{MAlign} are applied to facilitate visual local attribute mining. This introduces substantial improvements of **9.2%/9.2%** in Seen-Avg mAP/R@1 and **8.2%/9.2%** in Unseen-Avg mAP/R@1. These results validate that the proposed human attribute disentanglement design significantly enhances discriminative feature learning. Furthermore, when \mathcal{L}_{DAlign} is additionally employed, VLADR achieves **13.3%/13.3%** gains in Seen-Avg mAP/R@1 and **11.4%/13.2%** gains in Unseen-Avg mAP/R@1 over the baseline. These improvements demonstrate that the proposed continual attribute knowledge reinforcement mechanism effectively improves both domain adaptability and cross-domain generalization.

Ablation on hyperparameters: We further investigate the sensitivity of VLADR to the hyperparameters α and β , as shown in Fig. 6. The results indicate that the model

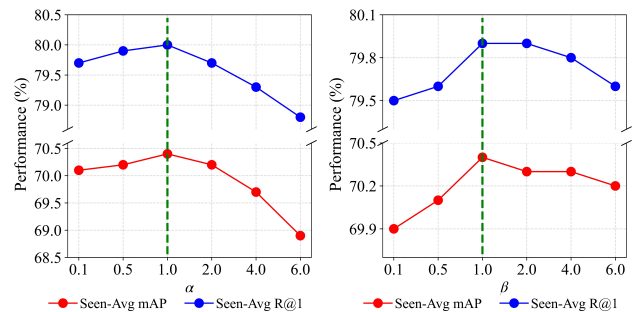


Figure 6. Ablation on hyperparameters.

maintains stable performance across a wide range of values, demonstrating strong robustness to hyperparameter fluctuations. In practice, we set both α and β to 1.0 by default based on empirical observations.

5. Conclusion

This paper presents VLADR, a novel VLM-driven LReID framework. The central idea is to explicitly model universally shared human attributes to improve both intra-domain knowledge learning and inter-domain knowledge transfer, thereby forming a continual attribute knowledge reinforcement paradigm. Specifically, VLADR introduces a Multi-grain Text Attribute Disentanglement mechanism to extract comprehensive global and diverse local textual attributes. Additionally, an Inter-domain Cross-modal Attribute Reinforcement scheme jointly performs cross-modal and inter-domain attribute alignment, enabling effective visual attribute mining and robust knowledge consolidation. This work demonstrates the strong potential of attribute-centric modeling in LReID and provides an efficient solution for fine-grained attribute knowledge discovery without imposing heavy annotation overhead.

Acknowledgements: This work was a research achievement of National Engineering Research Center of New Electronic Publishing Technologies, and was supported by the National Key R&D Program of China (2024YFA1410000), the National Natural Science Foundation of China (62376011, 62406313), and the Postdoctoral Fellowship Program of China Postdoctoral Science Foundation, Grant No. YJB20250283.

References

- [1] Home Office Scientific Development Branch. Imagery library for intelligent detection systems (i-lids). In *2006 IET conference on crime and security*, pages 445–448. IET, 2006. 5
- [2] Ying-Cong Chen, Xiatian Zhu, Wei-Shi Zheng, and Jian-Huang Lai. Person re-identification by camera correlation aware feature augmentation. *IEEE TPAMI*, 40(2):392–408, 2018. 2
- [3] Zhong Chen, Zhizhong Zhang, Xin Tan, Yanyun Qu, and Yuan Xie. Unveiling the power of clip in unsupervised visible-infrared person re-identification. In *ACM MM*, pages 3667–3675, 2023. 2
- [4] Zhenyu Cui, Jiahuan Zhou, Yuxin Peng, Shiliang Zhang, and Yaowei Wang. Dcr-reid: Deep component reconstruction for cloth-changing person re-identification. *IEEE TCSVT*, 33(8): 4415–4428, 2023. 2
- [5] Zhenyu Cui, Jiahuan Zhou, and Yuxin Peng. Dma: Dual modality-aware alignment for visible-infrared person re-identification. 19:2696–2708, 2024. 1
- [6] Zhenyu Cui, Jiahuan Zhou, Xun Wang, Manyu Zhu, and Yuxin Peng. Learning continual compatible representation for re-indexing free lifelong person re-identification. In *CVPR*, pages 16614–16623, 2024. 1
- [7] Zhenyu Cui, Jiahuan Zhou, and Yuxin Peng. Dkc: Differentiated knowledge consolidation for cloth-hybrid lifelong person re-identification. In *CVPR*, pages 3573–3582, 2025. 1
- [8] Wenhong Ge, Junlong Du, Ancong Wu, Yuqiao Xian, Ke Yan, Feiyue Huang, and Wei-Shi Zheng. Lifelong person re-identification by pseudo task knowledge preservation. In *AAAI*, pages 688–696, 2022. 1, 2
- [9] Yunpeng Gong, Liqing Huang, and Lifei Chen. Person re-identification method based on color attack and joint defence. In *CVPR*, pages 4313–4322, 2022. 1
- [10] Yunpeng Gong, Zhun Zhong, Yansong Qu, Zhiming Luo, Rongrong Ji, and Min Jiang. Cross-modality perturbation synergy attack for person re-identification. *NeurIPS*, 37: 23352–23377, 2024. 1
- [11] Douglas Gray and Hai Tao. Viewpoint invariant pedestrian recognition with an ensemble of localized features. In *ECCV*, pages 262–275. Springer, 2008. 5
- [12] Shuting He, Hao Luo, Pichao Wang, Fan Wang, Hao Li, and Wei Jiang. Transreid: Transformer-based object re-identification. In *ICCV*, pages 14993–15002. IEEE, 2021. 2
- [13] Martin Hirzer, Csaba Beleznai, Peter M Roth, and Horst Bischof. Person re-identification by descriptive and discriminative classification. In *Image Analysis*, pages 91–102. Springer, 2011. 5
- [14] Zhangyi Hu, Bin Yang, and Mang Ye. Empowering visible-infrared person re-identification with large foundation models. *NeurIPS*, 37:117363–117387, 2024. 2
- [15] Zhipeng Huang, Zhizheng Zhang, Cuiling Lan, Wenjun Zeng, Peng Chu, Quanzeng You, Jiang Wang, Zicheng Liu, and Zheng-jun Zha. Lifelong unsupervised domain adaptive person re-identification with coordinated anti-forgetting and adaptation. In *CVPR*, pages 14288–14297. IEEE, 2022. 4
- [16] Junnan Li, Dongxu Li, Silvio Savarese, and Steven Hoi. Blip-2: Bootstrapping language-image pre-training with frozen image encoders and large language models. In *ICML*, pages 19730–19742. PMLR, 2023. 6
- [17] Qiwei Li, Kunlun Xu, Yuxin Peng, and Jiahuan Zhou. Exemplar-free lifelong person re-identification via prompt-guided adaptive knowledge consolidation. *IJCV*, 132(11): 4850–4865, 2024. 2, 4, 5, 6
- [18] Siyuan Li, Li Sun, and Qingli Li. Clip-reid: exploiting vision-language model for image re-identification without concrete text labels. In *AAAI*, pages 1405–1413, 2023. 2, 4, 5, 6, 7, 8
- [19] Wei Li and Xiaogang Wang. Locally aligned feature transforms across views. In *CVPR*, pages 3594–3601. IEEE, 2013. 5
- [20] Wei Li, Rui Zhao, and Xiaogang Wang. Human reidentification with transferred metric learning. In *ACCV*, pages 31–44. Springer, 2012. 5
- [21] Wei Li, Rui Zhao, Tong Xiao, and Xiaogang Wang. Deep-reid: Deep filter pairing neural network for person re-identification. In *CVPR*, pages 152–159. IEEE, 2014. 5
- [22] Wei Li, Xiatian Zhu, and Shaogang Gong. Harmonious attention network for person re-identification. In *CVPR*, pages 2285–2294. IEEE, 2018. 2
- [23] Zhizhong Li and Derek Hoiem. Learning without forgetting. *IEEE TPAMI*, 40(12):2935–2947, 2017. 6
- [24] Zhizhong Li and Derek Hoiem. Learning without forgetting. *IEEE TPAMI*, 40(12):2935–2947, 2018. 2, 5, 6
- [25] Shibei Liu, Huijie Fan, Qiang Wang, Xiai Chen, Zhi Han, and Yandong Tang. Diverse representations embedding for lifelong person re-identification. *IEEE Transactions on Neural Networks and Learning Systems*, 2025. 5, 6
- [26] Zhaoshuo Liu, Zhiwei Guo, Chaolu Feng, Wei Li, Kun Yu, Jun Hu, and Jinzhu Yang. Tp-lreid: Lifelong person re-identification using text prompts. *Pattern Recognition*, page 112326, 2025. 4
- [27] Chen Change Loy, Tao Xiang, and Shaogang Gong. Time-delayed correlation analysis for multi-camera activity understanding. *IJCV*, 90(1):106–129, 2010. 5
- [28] Hao Luo, Youzhi Gu, Xingyu Liao, Shenqi Lai, and Wei Jiang. Bag of tricks and a strong baseline for deep person re-identification. In *CVPRW*, pages 0–0, 2019. 2
- [29] Yunyao Mao, Jiajun Deng, Wengang Zhou, Li Li, Yao Fang, and Houqiang Li. Clip4hoi: Towards adapting clip for practical zero-shot hoi detection. *NeurIPS*, 36:45895–45906, 2023. 2

- [30] Nan Pu, Wei Chen, Yu Liu, Erwin M Bakker, and Michael S Lew. Lifelong person re-identification via adaptive knowledge accumulation. In *CVPR*, pages 7897–7906. IEEE, 2021. 2, 6
- [31] Ergys Ristani, Francesco Solera, Roger Zou, Rita Cucchiara, and Carlo Tomasi. Performance measures and a data set for multi-target, multi-camera tracking. In *ECCV*, pages 17–35. Springer, 2016. 5
- [32] Jiangming Shi, Yachao Zhang, Xiangbo Yin, Yuan Xie, Zhizhong Zhang, Jianping Fan, Zhongchao Shi, and Yanyun Qu. Dual pseudo-labels interactive self-training for semi-supervised visible-infrared person re-identification. In *ICCV*, pages 11218–11228. IEEE, 2023. 1
- [33] Konstantin Shmelkov, Cordelia Schmid, and Karteek Alahari. Incremental learning of object detectors without catastrophic forgetting. In *ICCV*, pages 3420–3429, 2017. 2
- [34] Zhicheng Sun and Yadong Mu. Patch-based knowledge distillation for lifelong person re-identification. In *ACM MM*, pages 696–707, 2022. 2, 5, 6
- [35] Qizao Wang, Bin Li, and Xiangyang Xue. When large vision-language models meet person re-identification. *arXiv preprint arXiv:2411.18111*, 2024. 4
- [36] Zifeng Wang, Zizhao Zhang, Sayna Ebrahimi, Ruoxi Sun, Han Zhang, Chen-Yu Lee, Xiaoqi Ren, Guolong Su, Vincent Perot, Jennifer Dy, et al. Dualprompt: Complementary prompting for rehearsal-free continual learning. In *ECCV*, pages 631–648. Springer, 2022. 2
- [37] Longhui Wei, Shiliang Zhang, Wen Gao, and Qi Tian. Person transfer gan to bridge domain gap for person re-identification. In *CVPR*, pages 79–88. IEEE, 2018. 5
- [38] Guile Wu and Shaogang Gong. Generalising without forgetting for lifelong person re-identification. In *AAAI*, pages 2889–2897, 2021. 1, 2
- [39] Tong Xiao, Shuang Li, Bochao Wang, Liang Lin, and Xiaogang Wang. End-to-end deep learning for person search, 2016. 5
- [40] Kunlun Xu, Haozhuo Zhang, Yu Li, Yuxin Peng, and Jiahuan Zhou. Mitigate catastrophic remembering via continual knowledge purification for noisy lifelong person re-identification. In *ACM MM*, pages 5790–5799, 2024. 1, 2, 3
- [41] Kunlun Xu, Xu Zou, Yuxin Peng, and Jiahuan Zhou. Distribution-aware knowledge prototyping for non-exemplar lifelong person re-identification. In *CVPR*, pages 16604–16613. IEEE, 2024. 1, 2, 3, 4, 5, 6
- [42] Kunlun Xu, Xu Zou, and Jiahuan Zhou. Lstkc: Long short-term knowledge consolidation for lifelong person re-identification. In *AAAI*, pages 16202–16210, 2024. 1, 2, 3, 4, 5, 6
- [43] Kunlun Xu, Chenghao Jiang, Peixi Xiong, Yuxin Peng, and Jiahuan Zhou. Dask: Distribution rehearsing via adaptive style kernel learning for exemplar-free lifelong person re-identification. In *AAAI*, pages 8915–8923, 2025. 2, 5, 6
- [44] Kunlun Xu, Zichen Liu, Xu Zou, Yuxin Peng, and Jiahuan Zhou. Long short-term knowledge decomposition and consolidation for lifelong person re-identification. *IEEE TPAMI*, 2025. 1, 2, 5, 6
- [45] Kunlun Xu, Fan Zhuo, Jiangmeng Li, Xu Zou, and Jiahuan Zhou. Self-reinforcing prototype evolution with dual-knowledge cooperation for semi-supervised lifelong person re-identification. In *ICCV*, 2025. 5
- [46] Kunlun Xu, Xu Zou, Gang Hua, and Jiahuan Zhou. Componential prompt-knowledge alignment for domain incremental learning. In *ICML*, 2025. 1
- [47] Shan Yang and Yongfei Zhang. Mllmreid: multimodal large language model-based person re-identification. *arXiv preprint arXiv:2401.13201*, 2024. 4
- [48] Zexian Yang, Dayan Wu, Chenming Wu, Zheng Lin, Jingzi Gu, and Weiping Wang. A pedestrian is worth one prompt: Towards language guidance person re-identification. In *CVPR*, pages 17343–17353, 2024. 2
- [49] Chunlin Yu, Ye Shi, Zimo Liu, Shenghua Gao, and Jingya Wang. Lifelong person re-identification via knowledge refreshing and consolidation. In *AAAI*, pages 3295–3303, 2023. 2
- [50] Chenyu Zhang, Kunlun Xu, Zichen Liu, Yuxin Peng, and Jiahuan Zhou. Scap: Transductive test-time adaptation via supportive clique-based attribute prompting. In *CVPR*, pages 30032–30041, 2025. 1, 2
- [51] Haiyu Zhao, Maoqing Tian, Shuyang Sun, Jing Shao, Junjie Yan, Shuai Yi, Xiaogang Wang, and Xiaoou Tang. Spindle net: Person re-identification with human body region guided feature decomposition and fusion. In *CVPR*, pages 907–915. IEEE, 2017. 5
- [52] Liang Zheng, Liyue Shen, Lu Tian, Shengjin Wang, Jingdong Wang, and Qi Tian. Scalable person re-identification: A benchmark. In *ICCV*, pages 1116–1124. IEEE, 2015. 5
- [53] Jiahuan Zhou, Kunlun Xu, Fan Zhuo, Xu Zou, and Yuxin Peng. Distribution-aware knowledge aligning and prototyping for non-exemplar lifelong person re-identification. *IEEE TPAMI*, 2025. 2, 5, 6
- [54] Zijie Zhuang, Longhui Wei, Lingxi Xie, Tianyu Zhang, Hengheng Zhang, Haozhe Wu, Haizhou Ai, and Qi Tian. Rethinking the distribution gap of person re-identification with camera-based batch normalization. In *ECCV*, pages 140–157. Springer, 2020. 2